

Crystallization of Te–Si–Pb glasses exhibiting double T_g effect

M. LEONOWICZ, M. LASOCKA

Institute for Materials Science and Engineering, Warsaw Technical University, Narbutta 85, 02-524 Warsaw, Poland

Results of calorimetric, X-ray and transmission electron microscopy investigations of the glass–crystal transition in $\text{Te}_{80}\text{Si}_{20-x}\text{Pb}_x$ glasses are presented. The investigated glasses exhibit a double-stage crystallization and a double glass-transition temperature, T_g , within a composition range of 2.5 to 10 at % Pb. The second glass transition appears after partial crystallization of the glass. The double glass-transition phenomenon is discussed in relation to the crystallization process.

1. Introduction

Semiconducting glasses exhibit interesting electrical and optical properties [1–4]; most of these properties are connected with their crystallization processes. In many glasses, the glass–supercooled-liquid transition [5] precedes crystallization and is of importance on scientific and technological grounds. Changes in the glass transition temperature, T_g , after partial crystallization of glass have been found for several systems exhibiting multi-stage crystallization processes. A double T_g is seen for Te–Ge–Se [6], $\text{Te}_{80}\text{Ge}_{12.5}\text{Pb}_{7.5}$ [7] and $\text{Te}_{77}\text{Al}_{23}$ [8] glasses and for the metallic glass $(\text{Pd}_5\text{Ni}_5)_{1-y}\text{P}_y$ [9]. The above authors have related this phenomenon to phase separation taking place in the glass. The same explanation was proposed at the beginning of our experimental work [10] to account for the double T_g in $\text{Te}_{80}\text{Si}_{20-x}\text{Pb}_x$ glasses. Further investigations, however, have not confirmed these predictions.

The detection of phase separation in a glass is sometimes very difficult since phase separation may produce only subtle changes in the diffraction pattern, whereas changes in the microstructure are evident only if the separating phases markedly differ in electron density. For binary glasses a composition-independent T_g is evidence of phase separation. In multi-component systems, the interpretation of the same effect is much more difficult and requires the use of several experimental techniques.

The aim of this work was to elucidate the T_g

changes in $\text{Te}_{80}\text{Si}_{20-x}\text{Pb}_x$ glasses in the light of thermally-induced structural transformations.

2. Experimental procedure

For preparation of $\text{Te}_{80}\text{Si}_{20-x}\text{Pb}_x$ glasses high-purity (99.999% and 99.9999% purity) elemental solids were used; x was varied at intervals of 2.5 at%. Samples were melted under vacuum in quartz ampoules. The alloys so prepared were remelted and rapidly cooled by the gun technique [11].

Calorimetric measurements were carried out using a Perkin–Elmer DSC-2 unit at a rate of 20°min^{-1} . The melting point of an In sample, measured under conditions of the experiment, was used for temperature calibration. For measurement of the second T_g the procedure proposed by Lasocka [7] was applied. Samples were heated in a calorimeter until the end of the first crystallization step was reached and then they were rapidly cooled and reheated until complete crystallization had taken place. For the isothermal measurements, the fraction of material crystallized after a time, τ , at temperature T was evaluated by integration of the area enclosed between the experimental curve and the base line.

The phases present after heating were determined using X-ray diffraction analysis (using $\text{CuK}\alpha$ radiation).

The structure was examined in a Phillips 100 kV transmission electron microscope. The as-quenched samples were observed, without thinning, using electron beam heating.

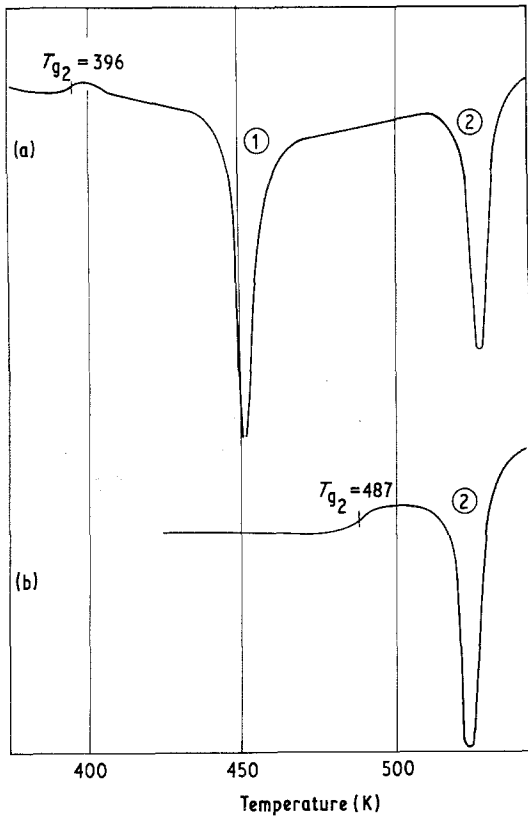


Figure 1 Differential scanning calorimetry (DSC) traces taken for $\text{Te}_{80}\text{Si}_{12.5}\text{Pb}_{7.5}$ glass. Heating rate, $20^\circ \text{ min}^{-1}$; dH/dT , 2 mcal sec^{-1} and sample weight, 10 mg. (a) Continuous heating until complete crystallization and (b) heating until the end of the first crystallization step followed by cooling and reheating.

3. Results

3.1. Calorimetric results

$\text{Te}_{80}\text{Si}_{20-x}\text{Pb}_x$ glasses exhibit, within the composition range of 2.5 to 10 at % Pb, two separate crystallization effects and a double T_g . The second glass transition temperature, T_{g_2} , appears in the

TABLE I. Crystallization and glass transition temperatures (in K) of $80 \text{ at } \% \text{ Te}-(20-x) \text{ at } \% \text{ Si}-x \text{ at } \% \text{ Pb}$ glasses.

x	$T_{g_1}^*$	$T_{g_2}^*$	$T_{x_1}^\dagger$	$T_{x_2}^\dagger$
0.0	430	—	489	561
2.5	421	520	503	547
5.0	408	510	473	524
7.5	396	487	446	523
10.0	386	469	433	486
12.5	377	—	412	449
15.0	361	—	380	384
17.5	349	—	369	—
20.0	330	—	337	—

* T_{g_1} and T_{g_2} are the first and second glass transition temperatures, respectively.

† T_{x_1} and T_{x_2} are the crystallization temperatures of the first and the second stages, respectively.

second heating of the sample, which was previously heated up to the end of the first crystallization step and then cooled. In this second heating, the first exothermic effect of crystallization and T_{g_1} disappear (Fig. 1). An increase in the Pb concentration lowers the glass transition and crystallization temperatures (Fig. 2). Experimental data concerning glass transition and crystallization temperatures are recorded in Table I. The linear dependence of T_{g_1} and T_{g_2} on the composition indicate that these temperatures correspond to solutions of different composition in every glass of the system.

Kinetics of crystallization were determined for the $\text{Te}_{80}\text{Si}_{17.5}\text{Pb}_{2.5}$ glass. The fractions of material crystallized after a time, τ , at temperature T , $X_T(\tau)$, for the first and second transformations, are plotted in Figs 3a and 4a, respectively. The nucleation and growth rates for the investigated glass were predicted using the Avrami equation [12]:

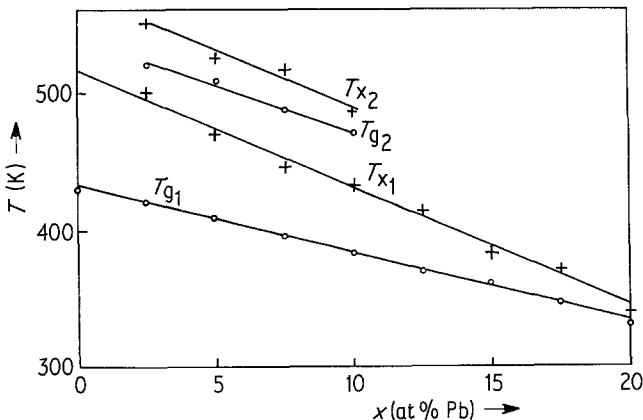


Figure 2 Glass transition and crystallization temperatures plotted against composition.

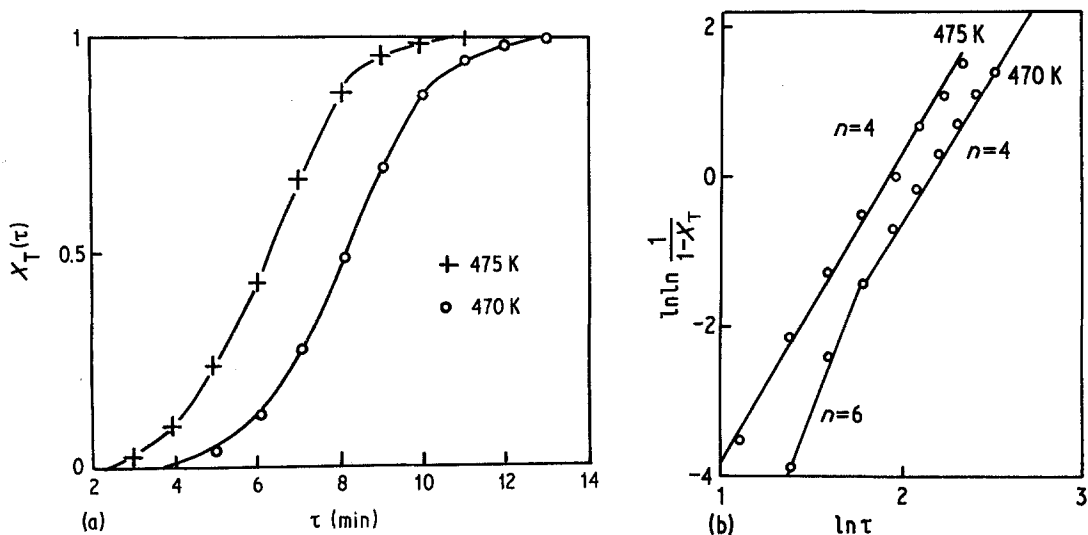


Figure 3 The first stage of crystallization of $\text{Te}_{80}\text{Si}_{17.5}\text{Pb}_{2.5}$ glass. (a) Transformed volume as a function of annealing time and (b) prediction of the index n from Equation 2.

$$X_T(\tau) = 1 - \exp(-k\tau)^n, \quad (1)$$

where $X_T(\tau)$ is the fraction of material transformed after a time τ , k is related to the rates of nucleation and growth and n is a constant dependent on nucleation and the growth mechanism. For isothermal conditions, the Avrami equation can be rearranged to the form

$$\ln [\ln (1/1 - X_T)] = C + n \ln \tau \quad (2)$$

$\ln [\ln (1/1 - X_T)]$ is plotted against $\ln \tau$ for the first and second stages of crystallization in Figs 3b and 4b, respectively. $n = 4$, for the first stage of crystallization (Fig. 3b), can be interpreted to indicate diffusion-limited growth with increasing

nucleation rate [13]. At 470 K two different values of n are observed. This phenomenon can be due to the effects of phase separation prior to crystallization. It is plausible that the processes of the second crystallization step ($n = 3$ to 5) are interface controlled with the constant growth rate at 520 K [13].

3.2. X-ray and microscopic results

The aim of the diffractometric investigations was to determine the phases present after each stage of crystallization. Some suggestions presented in [10] are not, at present, completely confirmed. From the detailed measurements in this work:

(a) after the first crystallization step Te crystals

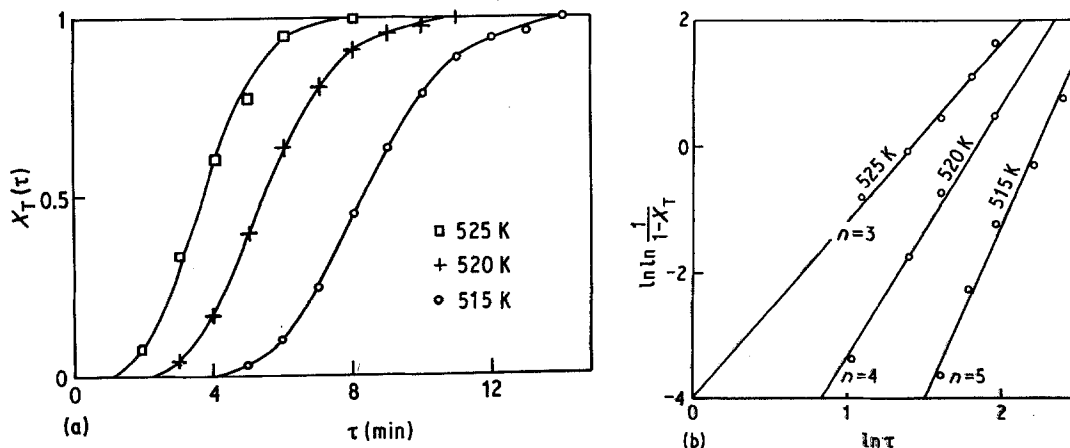


Figure 4 The second stage of crystallization of $\text{Te}_{80}\text{Si}_{17.5}\text{Pb}_{2.5}$ glass. (a) Transformed volume as a function of annealing time and (b) prediction of the index n from Equation 2.

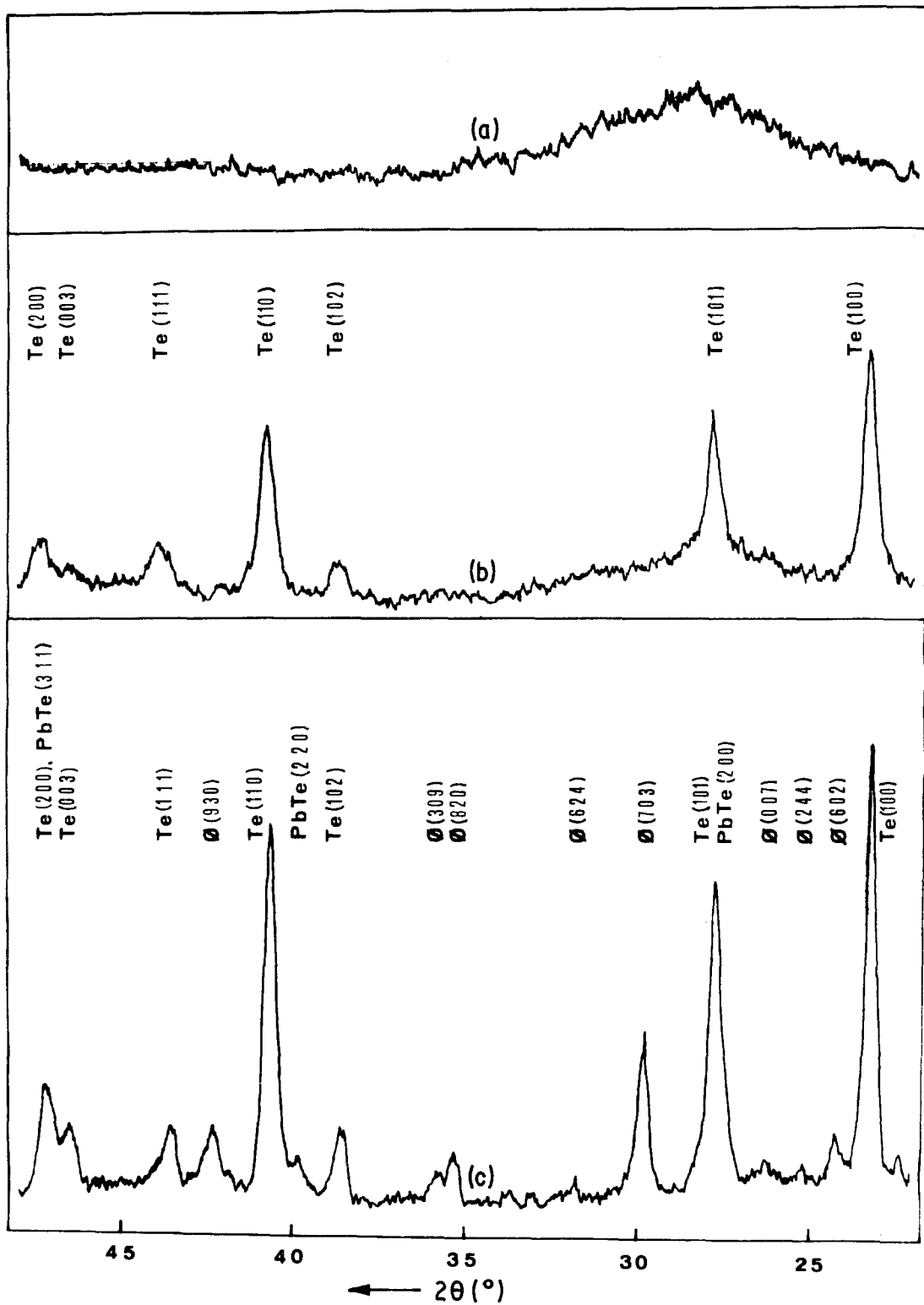


Figure 5 Diffraction pattern of $\text{Te}_{80}\text{Si}_{17.5}\text{Pb}_{2.5}$ alloy. (a) Glass, (b) after the first crystallization and (c) after complete crystallization.

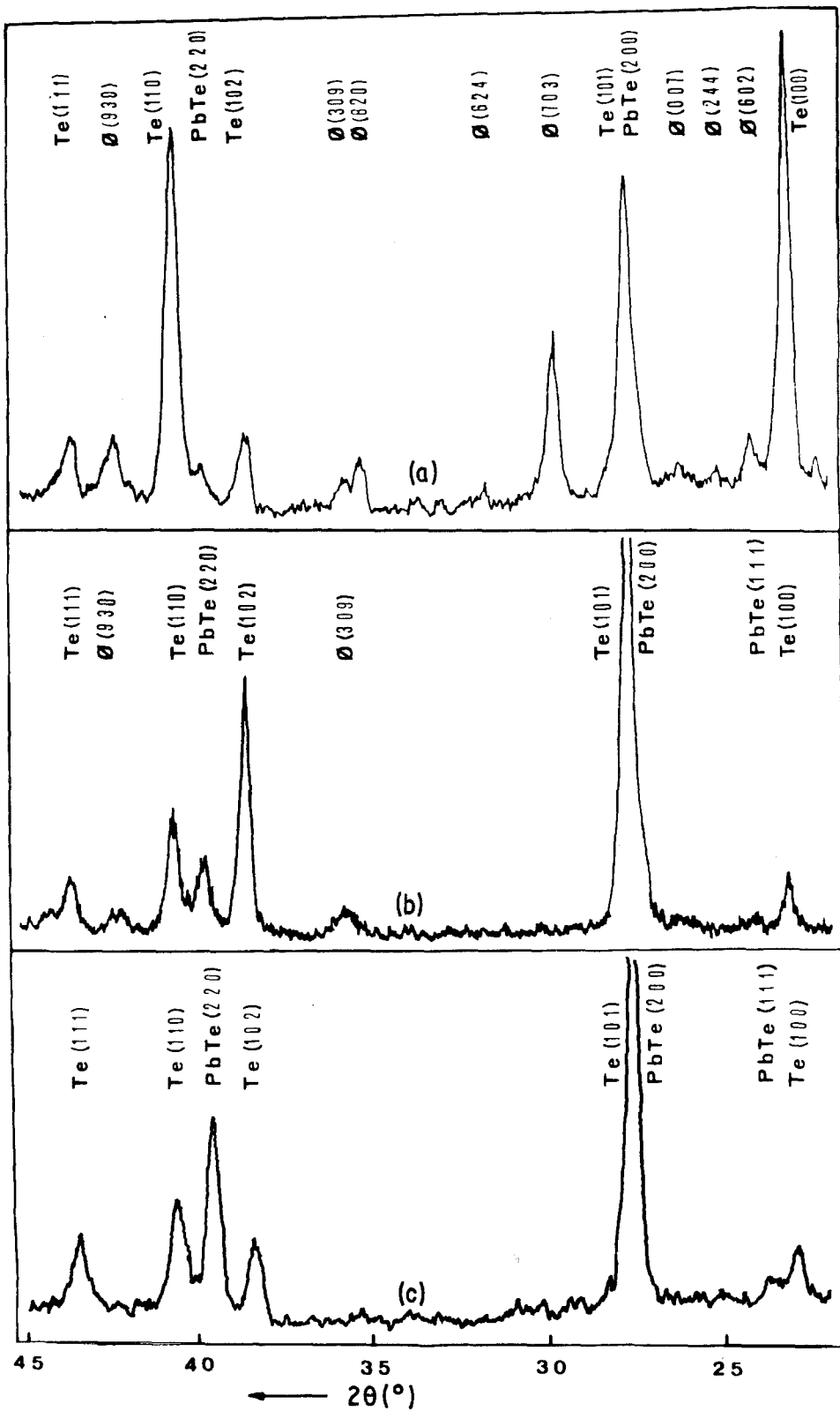


Figure 6 Diffraction patterns of crystalline $\text{Te}_{80}\text{Si}_{20-x}\text{Pb}_x$ alloys for (a) $x = 2.5$ at % Pb, (b) $x = 7.5$ at % Pb and (c) $x = 10$ at % Pb.

are present;

(b) after complete crystallization, Te, PbTe, and a phase, denoted as ϕ (of hexagonal structure and lattice parameters of $a = 6a_{\text{Te}}$ and $c = 4c_{\text{Te}}$) are present.

As an example, the crystallization products of $\text{Te}_{80}\text{Si}_{17.5}\text{Pb}_{2.5}$ glass is shown in Fig. 5. The intensity and number of reflections attributable to the ϕ -phase increase with increasing Si concentration (Fig. 6), so characterizing the phase as a solid solution of Si in Te.

Transmission electron microscopy investigations afforded complementary data to the X-ray measurements and showed the morphology of phases. The crystallization scheme of glasses exhibiting a double T_g is exemplified in Fig. 7 for $\text{Te}_{80}\text{Si}_{10}\text{Pb}_{10}$ glass. Fig. 7a shows a typical homogeneous amorphous structure. The first phase to appear is crystalline tellurium with a dendritic morphology, shown in Fig. 7b. Further heating leads to eutectoid crystallization of the remaining amorphous matrix, shown in Fig. 7c. All the glasses investigated exhibit a similar morphology of crystallization, but the higher the lead concentration, the more fine-grained is the structure.

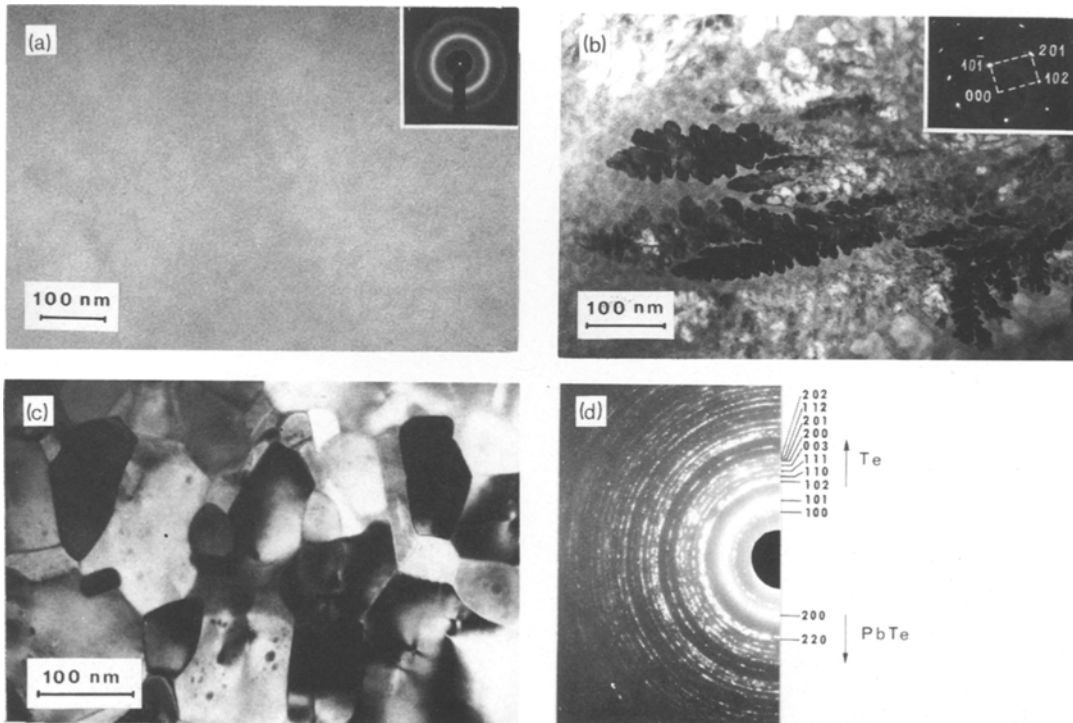


Figure 7 Micrographs of $\text{Te}_{80}\text{Si}_{10}\text{Pb}_{10}$ glass at various stages of crystallization. (a) Glass (inset shows electron diffraction pattern), (b) beginning of crystallization showing dendritic crystals of tellurium (inset shows electron diffraction pattern), (c) crystalline structure and (d) diffraction pattern of crystalline structure (the lack of reflections from the ϕ phase is a result of the small amount of this phase present in the alloy).

4. Discussion

Double-stage crystallization of glasses within the composition range 2.5 to 10 at % Pb points to phase separation occurring in the material. The question arises as to when the segregation occurs. Crystallization of tellurium at the beginning of the transformation process brings about a change in the T_g value. Composition-dependent changes in T_{g1} exclude the possibility of a relationship between this temperature and the glass–melt transformation of amorphous tellurium. From the observations it seems reasonable that T_{g1} can be the glass–melt transition temperature of the homogeneous ternary glass. The homogeneity of the glass is also confirmed by transmission electron microscopy (Fig. 7a).

Phase separation occurs in the melt with instantaneous crystallization of precipitated tellurium. The alloy, cooled from this point, is a glass-ceramic [14] consisting of dendrites of tellurium in an amorphous matrix (Fig. 7b). T_g is considered to be the glass–melt transformation temperature of the amorphous material remaining after crystallization of tellurium. A rise of the T_g value with a decrease in Te content in a glass is confirmed by

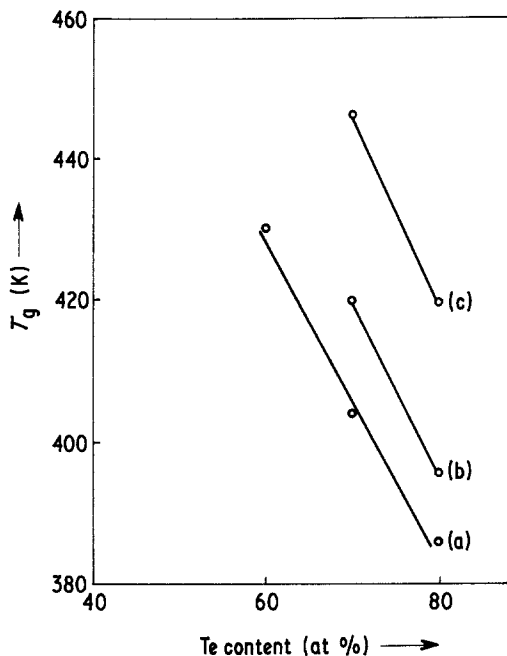


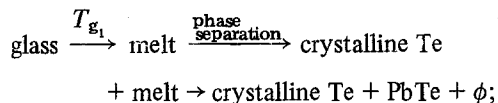
Figure 8 (a-c) Glass transition temperatures plotted against Te content for molar ratios $N_{\text{Si}}/N_{\text{Pb}}$ of 1, 1.66 and 7, respectively. (a) $\text{Te}_x\text{Si}_y\text{Pb}_7y$, (b) $\text{Te}_x\text{Si}_y\text{Pb}_{1.66y}$ and (c) $\text{Te}_x\text{Si}_y\text{Pb}_7y$.

investigations of T_{g_2} changes as a function of Te concentration in glasses with constant molar ratio $N_{\text{Si}}/N_{\text{Pb}}$, where N_{Si} and N_{Pb} are the molar concentrations of Si and Pb, respectively (Fig. 8).

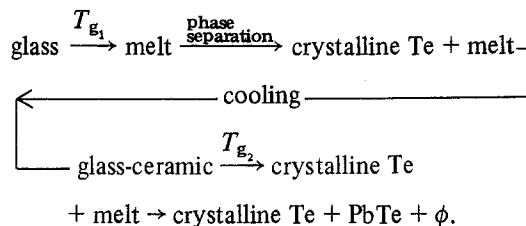
The present results suggest the following courses of transformation in $\text{Te}_{80}\text{Si}_{20-x}\text{Pb}_x$ glasses:

(a) Composition range 2.5 to 10 at% Pb. For this composition range there are two possible schemes of transformation.

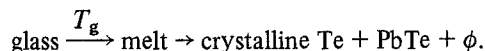
(i) Continuous heating:



(ii) cooling after the first crystallization stage and reheating:



(b) Composition range 12.5 to 17.5 at% Pb. For this composition range the scheme of transformation is as follows.



References

1. N. F. MOTT and E. A. DAVIS, "Electronic Processes in Non-Crystalline Materials" (Pergamon Press, Oxford, 1971) pp. 188-398.
2. R. GRIGOROVICI, *Thin Solid Films* 9 (1971) 1.
3. J. R. BOSNELL, *Phys. Technol.* 4 (1973) 113.
4. K. WEISER, *Prog. Sol. Stat. Chem.* 11 (1976) 403.
5. H. S. CHEN, *Sci. Rep. RITU* 27 (1979) 97.
6. D. J. SARRACH and J. P. De NEUFVILLE, *J. Non-Cryst. Sol.* 22 (1976) 245.
7. M. LASOCKA, *J. Mater. Sci.* 13 (1978) 2055.
8. J. COLMENERO and J. M. BARANDARIAN, *J. Non-Cryst. Sol.* 30 (1979) 263.
9. H. S. CHEN, *Mater. Sci. Eng.* 23 (1976) 151.
10. M. LEONOWICZ and M. LASOCKA, *J. Mater. Sci.* 15 (1980) 1586.
11. M. CHYCZEWSKI and H. MATYJA, Institute of Nuclear Research, Report Number 1343/XIV/PS, Warsaw, 1979.
12. M. AVRAMI, *J. Phys. Chem.* 9 (1941) 177.
13. J. W. CHRISTIAN, "The Theory of Transformation in Metals and Alloys" (Pergamon Press, Oxford, 1964) p. 489.
14. W. HINZ, in "Glass '77" Vol. 1, edited by J. Götz (CVTS Dum Techniky, Praha, 1977) pp. 217-260.

Received 22 January and accepted 19 February 1981.